Phase-tunable Josephson junction and spontaneous mass current in a spin-orbit-coupled Fermi superfluid

Lei Jiang,[1] Yong Xu,[1,2] and Chuanwei Zhang[1]
[1]*Department of Physics, The University of Texas at Dallas, Richardson, Texas 75080, USA*
[2]*Department of Physics, University of Michigan, Ann Arbor, Michigan 48109, USA*
(Received 13 July 2016; published 13 October 2016)

Atomtronics has the potential for engineering new types of functional devices, such as Josephson junctions (JJs). Previous studies have mainly focused on JJs whose ground states have zero or π superconducting phase difference across the junctions, while arbitrary phase-tunable JJs may have important applications in superconducting electronics and quantum computation. Here we show that a phase-tunable JJ can be implemented in a spin-orbit-coupled cold atomic gas with the magnetic tunneling barrier generated by a spin-dependent focused laser beam. We consider the JJ confined in either a linear harmonic trap or a circular ring trap. In the ring trap, the magnetic barrier induces a spontaneous mass current for the ground state of the JJ, demonstrating the magnetoelectric effects of cold atoms.

DOI: 10.1103/PhysRevA.94.043625

I. INTRODUCTION

Atomtronics is a new exciting interdisciplinary field [1–4] aiming to mimic electronic circuits and build new functional devices, utilizing the high controllability and purity of cold atomic gases. Recently, atomic Josephson junctions (JJs) have been realized [5–7] in toroidal Bose-Einstein condensates (BECs) [8–11], analogous to the well-known superconducting quantum interference devices. In solid-state devices, besides the common zero phase, the ground state of a JJ may possess a π phase of the superconducting order parameter across the junction [12], which can be generated by inserting a layer of insulator with magnetic impurities [13] or a layer of ferromagnetic material [14] or an unconventional superconductor [15,16] between two regular s-wave superconductors. Such π-phase JJs resemble the Larkin-Ovchinnikov (LO) state in a spin-imbalanced superconductor [17] and have also been studied in cold atomic gases [18,19]. More generally, the phase of the JJ ground state could be arbitrary (not zero or π), which may have important applications such as phase batteries and rectifiers [20,21], phase-based quantum bits [22], etc. Recently, such arbitrary-phase JJs have been experimentally realized using nanowire quantum dots [23]. However, arbitrary-phase JJs have not been explored in atomtronics.

In cold atomic gases, synthetic gauge fields and spin-orbit coupling have paved the way for neutral atoms to interact with external synthetic electric and magnetic fields [24–32]. In particular, one-dimensional (1D) equal-Rashba-Dresselhaus spin-orbital coupling was realized experimentally for fermions using a two-photon Raman process [30–32]. Interestingly, in the presence of Raman detuning, which acts as an in-plane Zeeman field, the inversion symmetry of the Fermi surface is broken, leading to the Fulde-Ferrell (FF) superfluid [33] with a spatially modulating phase of the order parameter [34–41]. Therefore a nature question is whether such a spatially modulating phase of the FF state could be used to engineer JJs with arbitrary and tunable phases.

In this article, we address this issue by studying a JJ generated by a magnetic barrier in a 1D spin-orbit-coupled Fermi superfluid. We consider two types of traps: a linear harmonic trap and a circular ring trap. For the former, the spin-momentum coupling has been experimentally realized for Fermi gases [30–32], and for the latter, the corresponding spin–orbital-angular-momentum (SOAM) coupling was proposed [42–47] to be realized using Laguerre-Gaussian (LG) laser beams [48–51] (see Fig. 1). The magnetic barrier for the JJ can be generated by a spin-dependent focused laser beam. In both types of traps, the phase across the JJ can be continuously tuned by changing the parameters of the magnetic barrier. Interestingly, we find that the magnetic barrier induces a spontaneous finite-mass current for the ground state of the JJ in a ring trap, which realizes the magnetoelectric effects in atomtronics.

II. MODEL

For simplicity of the numerical calculation, hereafter we consider 1D Fermi gases, but the results apply to two and three dimensions due to the same mechanism for generating the FF phase junction. We first consider a spin-momentum-coupled Fermi gas confined in a 1D harmonic trap. Within the mean-field approximation, the dynamics of the system is governed by the mean-field many-body Hamiltonian

$$H = \int dx\{\hat{\Psi}^{+} H_S \hat{\Psi} - [\Delta(x)\hat{\psi}_{\uparrow}^{+}\hat{\psi}_{\downarrow}^{+} + \text{H.c.}]\}, \qquad (1)$$

where $\hat{\Psi} = (\hat{\psi}_{\uparrow}(x), \hat{\psi}_{\downarrow}(x))^{T}$ and $\hat{\psi}_{\sigma}(x)$ with $\sigma = \uparrow, \downarrow$ are fermionic annihilation operators for the spin σ state. The single-particle Hamiltonian $H_S = H_0 + H_{\text{SOC}} + H_Z$. $H_0 = [-\frac{\hbar^2\partial^2}{2m\partial x^2} - \mu + \frac{m\omega^2 x^2}{2}]$, with the Planck constant $\hbar$, the mass of atoms m, the chemical potential μ, and the harmonic trap frequency ω. The spin-momentum-coupling term $H_{\text{SOC}} = -i\lambda\sigma_z\partial_x$, with Pauli matrices $\sigma_{i=x,y,z}$ and coupling strength $\lambda = \hbar^2 k_R/m$, where k_R is the recoil momentum of the Raman laser. The Zeeman field term $H_Z = -\Omega_R\sigma_x + V_Z(x)\sigma_z$, with Ω_R and $V_Z(x)$ being the out-of-plane and in-plane Zeeman field strengths. Ω_R is determined by the Raman laser intensities, and $V_Z(x)$ is induced by the local magnetic barrier. The order parameter $\Delta(x) \equiv -g_{1D}\langle\hat{\psi}_{\downarrow}(x)\hat{\psi}_{\uparrow}(x)\rangle$. The constant g_{1D} is the 1D two-body s-wave interaction strength, which can

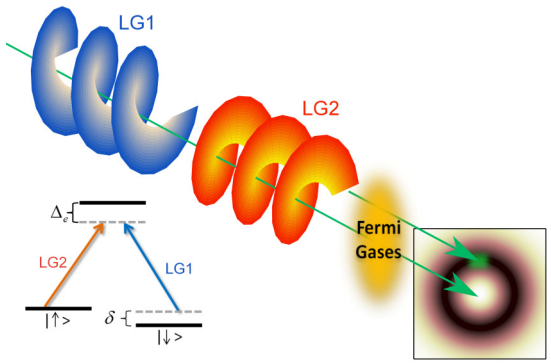

FIG. 1. Illustration of the proposed experimental setup. Two copropagating LG beams (LG1 and LG2) with different orbital angular momenta couple two atomic hyperfine states in the ring structure to induce SOAM coupling through the Raman process. An additional spin-dependent focused laser beam provides a local magnetic barrier (the green spot).

be characterized by a scaleless parameter $\gamma \equiv -mg_{1D}/(\hbar^2 n_0)$ that represents the ratio between the interaction and kinetic energies. Here $n_0 = (2/\pi)\sqrt{Nm\omega/\hbar}$, with N being the total number of atoms.

In terms of the Nambu spinor $\hat{\Phi}(x) = [\hat{\psi}_\uparrow(x), \hat{\psi}_\downarrow(x), \hat{\psi}^+_\uparrow(x), \hat{\psi}^+_\downarrow(x)]^T$, the mean-field Hamiltonian $H = \frac{1}{2}\int dx\, \hat{\Phi}^+(x) H_{\rm BdG} \hat{\Phi}(x)$ can be numerically solved using the hybrid self-consistent Bogoliubov–de Gennes (BdG) method [52–54]. The BdG quasiparticles are obtained by diagonalizing

$$H_{\rm BdG}\, \varphi_\eta(x) = E_\eta\, \varphi_\eta(x)\,, \tag{2}$$

with energies E_η and wave functions $\varphi_\eta(x) = [u_{\uparrow\eta}(x), u_{\downarrow\eta}(x), v_{\uparrow\eta}(x), v_{\downarrow\eta}(x)]^T$ indexed by subscript $\eta = 1,2,3,\cdots$. The wave functions are normalized such that $\sum_{\sigma=\uparrow,\downarrow}\int dx[|u_{\sigma\eta}(x)|^2 + |v_{\sigma\eta}(x)|^2] = 1$.

We use the "hybrid" method of Refs. [52,53] to solve the eigenvalue problem of Eq. (2). We get all eigenenergy pairs of $H_{\rm BdG}$ with energy $|E| \leqslant E_c$, where E_c is a cutoff energy that is chosen to be large compared to the Fermi energy but small compared to the width of the discretized $H_{\rm BdG}$ spectral. Typically, we take $E_c = 8E_F$ with the noninteracting Fermi energy $E_F = \hbar\omega N/2$ in a harmonic trap. The Fermi wave number k_F is obtained from $E_F = \hbar^2 k_F^2/2m$, and the Thomas-Fermi radius $x_{\rm TF} = \sqrt{N\hbar/(m\omega)}$. For this eigenstate problem, we use the discrete-variable representation (DVR) of the plane-wave basis [55]. The order parameter is

$$\Delta(x) = -\frac{g_{1D}}{2}\sum_\eta [u_{\uparrow\eta} v^*_{\downarrow\eta} f(E_\eta) + u_{\downarrow\eta} v^*_{\uparrow\eta} f(-E_\eta)], \tag{3}$$

where $f(E)$ is the Fermi-Dirac distribution function $f(E) = 1/[e^{E/k_BT} + 1]$ and T is the temperature. Here we present results for $T = 0$. For states above the energy cutoff E_c, we employ a semiclassical method based on the local-density approximation. The new order parameter is calculated by combining the contributions from the DVR and semiclassical solutions and is put back in the mean-field Hamiltonian. The procedure is repeated until the order parameter converges.

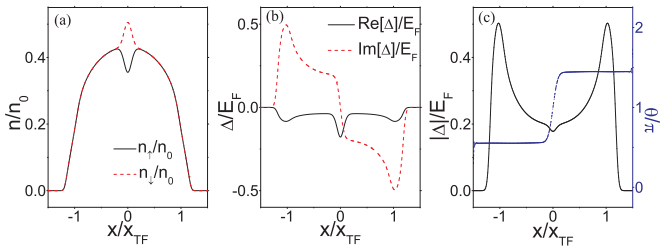

FIG. 2. Phase-tunable Josephson junctions in a 1D harmonic trap. The magnetic barrier is located at the center of the harmonic trap. (a) Atomic density profiles. (b) The real and imaginary parts of the order parameter. (c) The absolute value and phase of the order parameter. $u_{\rm mag} = 0.05E_F x_{TF}, a_{\rm imp} = 0.1x_{TF}$, $\gamma = 2.2$, $\lambda = 1.5E_F/k_F, \Omega_R = 0.8E_F, \mu = 0.285E_F, N = 60$.

In the ring trap, the corresponding SOAM coupling is realized by two LG Raman lasers with opposite orbital angular momenta ($L_1 = -L_2 = L$) [44–47] (Fig. 1). The Hamiltonian is similar, except there is no harmonic trap and x is changed to $R\theta$, where R is the radius of the ring. The azimuth angle θ is in the range $\theta \in [-\pi, \pi]$. The SOAM coupling strength is $\lambda = \hbar^2 L/mR$.

III. PHASE-TUNABLE JOSEPHSON JUNCTION

We first consider a magnetic barrier for the JJ located at the center of the harmonic trap and generated by a spin-dependent focused laser beam with $V_Z(x) = u_{\rm mag} e^{-(\frac{x}{a_{\rm mag}})^2}/a_{\rm mag}\sqrt{\pi}$, where $u_{\rm mag} > 0$ and $a_{\rm mag}$ are barrier strength and width, respectively. In the absence of the magnetic barrier, the system is population balanced, and the density exhibits a parabolic profile which can be described by the Thomas-Fermi approximation. In the presence of a local magnetic barrier, the density exhibits a dip for spin-↑ atoms (solid black line) and a bump for spin-↓ ones (dashed red line) at the center of the trap [as shown in Fig. 2(a)] because of opposite potentials for the two spins.

The magnetic barrier acts as a local in-plane Zeeman field and induces the local FF type of order parameter, as shown in Fig. 2(b), where both real (solid black line) and imaginary (dashed red line) parts of the order parameter are nonzero. In Fig. 2(c), we plot the absolute value of the order parameter (solid black line), showing a small dip inside the barrier due to the suppression of Cooper pairing by the local Zeeman field. The order parameter also exhibits two maxima near the edge of the Fermi cloud, which is a unique feature in the 1D case [52]. Remarkably, the phase of the order parameter (dashed blue line) changes linearly (the property of the FF type of order parameter) inside the barrier and remains constant outside, as shown Fig. 2(c). The constant values of the phases are different on the left and right sides of the barrier and can be any value, demonstrating a JJ with tunable phase. In a two-dimensional (2D) system separated by a magnetic barrier chain, such a phase junction still exists.

Such a tunable phase across the magnetic barrier also exists inside a ring trap. However, the phase outside the barrier is not constant anymore due to the periodic confinement. To clearly distinguish the phase change in the barrier from the bulk region, we consider a rectangular-shaped barrier located at

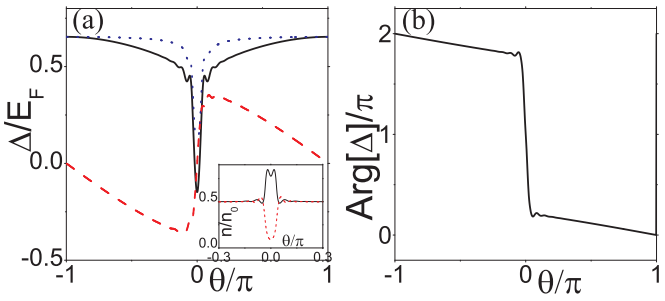

FIG. 3. Phase-tunable JJ in a ring. (a) The real part (solid black line), imaginary part (dashed red line), and absolute value of the order parameter (dotted blue line). Inset: Density profiles for $|\uparrow\rangle$ state (solid black line) and $|\downarrow\rangle$ state (dashed red line). (b) The phase of the order parameter. In numerical calculation, we take the radius $R = 1, \hbar = 1$. The noninteracting Fermi momentum is defined as $k_F = \pi n_0/2$, and the Fermi energy $E_F = \hbar^2 k_F^2/2m$, with $n_0 = N/2\pi R$ being the average density. The parameters are $\lambda = 2.3E_F/k_F, \gamma = 2.4, \Omega_R = 0.8E_F, \delta = 0.25E_F, u_{\rm mag} = 1.5E_F, a_{\rm mag} = 0.1, \mu = -0.41E_F$ and $N = 60$.

$\theta = 0$, described by $V_Z(\theta) = -u_{\rm mag}[\Theta(\theta + a_{\rm mag}) - \Theta(\theta - a_{\rm mag})]$, with the step function $\Theta(x)$. We have studied realistic Gaussian potentials, and the results are qualitatively the same with a small quantitative deviation from the rectangular one. In Fig. 3, we present our self-consistent BdG results. Similar to the harmonic trap case, in Fig. 3(a), there is a local imbalanced region inside the barrier (the inset) where both real and imaginary parts of the order parameter are nonzero and have different structures. More interestingly, as shown in Fig. 3(b), the phase of the order parameter outside the barrier changes almost linearly, instead of being constant, due to the periodic boundary condition.

The phase difference across the JJ can be continuously tuned. In Fig. 4(a), we present three different phase structures for three different barrier strengths $u_{\rm mag}$. To quantitatively characterize the phase change, we introduce two types of phase differences: $\varphi_{\rm dif} = \phi_L - \phi_R$ between two edges of the barrier and the phase change φ_{JJ} outside the barrier. To avoid the complication from the periodicity of the phase angle, we treat

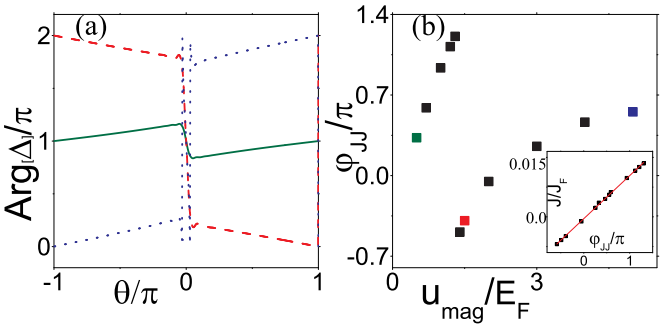

FIG. 4. (a) The phase structure of the order parameter in the real space with different barrier strengths. (b). Tunable phase of the JJ vs barrier strength. The three colored squares correspond to the three cases in (a). Inset: Spontaneous mass current as a function of the phase of the JJ. Mass current is in units of $J_F = n_0 v_F$, where v_F is the Fermi velocity $v_F = \hbar k_F/m$.

the order parameter phase in its principal value of $[0, 2\pi)$. With increasing barrier strength, $\varphi_{\rm dif}$ increases from less than π to larger than π but smaller than 2π and finally to even larger than 2π. Obviously, for small barrier strengths, $\varphi_{JJ} = \varphi_{\rm dif} > 0$; for moderate ones, $\varphi_{JJ} = \varphi_{\rm dif} - 2\pi < 0$, and for strong ones, $\varphi_{JJ} = \varphi_{\rm dif} - 2\pi > 0$. In Fig. 4(b), we plot φ_{JJ} as a function of the magnetic barrier strength. φ_{JJ} has a discontinuous point near $\varphi_{JJ} = 1.2\pi$. In fact, when $\varphi_{\rm dif}$ is around π, there are two steady states corresponding to positive and negative φ_{JJ}, respectively. When $\varphi_{\rm dif} > 1.2\pi$, the state with negative φ_{JJ} has lower energy and becomes the ground state. We note that the phase difference of the JJ can also be tuned by changing other parameters such as the barrier width and the atom-atom interaction strength.

IV. SPONTANEOUS MASS CURRENT

The linear phase gradient outside the barrier of the JJ induces a spontaneous mass current in the ring trap, which is defined as

$$J(\theta) = \frac{\hbar}{mR} \sum_{\sigma=\uparrow,\downarrow} \mathrm{Re}\langle \psi_\sigma^\dagger(\theta)(-i\partial_\theta + L_\sigma)\psi_\sigma(\theta)\rangle. \quad (4)$$

Here $L_\uparrow = -L_\downarrow = L$, and the second term originates from the SOAM coupling. The mass current is zero for the linear 1D system in the harmonic trap, where there is no phase gradient outside the barrier. The inset of Fig. 4(b) shows that the ground state of the JJ with finite φ_{JJ} exhibits a finite-mass current, which is linearly proportional to φ_{JJ}. Such a magnetic-barrier-induced mass current demonstrates the magnetoelectric effect of cold atoms, which may have important applications in atomtronics.

The tunable phase across the barrier and the spontaneous mass current along the ring could be understood from the FF order parameter of the superfluid in the presence of SOAM coupling and in-plane Zeeman field. Here we illustrate this mechanism by considering a uniform in-plane Zeeman field along the whole ring [i.e., $V_Z(\theta) = \delta$]. We find the ground state of the system possesses finite-angular-momentum Cooper pairs $\Delta(\theta) = \Delta_0 \exp(i l_0 \theta)$, with Δ_0 being constant and l_0 being an integer due to the periodic boundary condition. To obtain the order parameter numerically, we start from random initial order parameters and then self-consistently solve the BdG equation in the real space until it converges. We find that each converged final state always corresponds to a state with certain l, suggesting that these states are steady states. To see this more clearly, we choose $\Delta(\theta) = \Delta_0 \exp(il\theta)$ and compute the thermodynamic potential for each l with fixed chemical potential as a function of $|\Delta(\theta)|$. In the mean-field theory, the thermodynamic potential Ω is defined as $\Omega = \langle H \rangle - \int R d\theta\, |\Delta(\theta)|^2/g_{1D}$, which can be expanded in the angular momentum space (similar to the momentum space in a traditional homogeneous 1D system). In Fig. 5(a), we plot the thermodynamic potential with respect to $|\Delta(\theta)|$ for different l, showing that there always exists a local minimum of the thermodynamic potential for each l, and we find that the converged state obtained with the self-consistent calculation in the real space exactly corresponds to the local minimum for each l. The ground state is the one with the lowest thermodynamic potential and $l_0 = 3$ for the particular

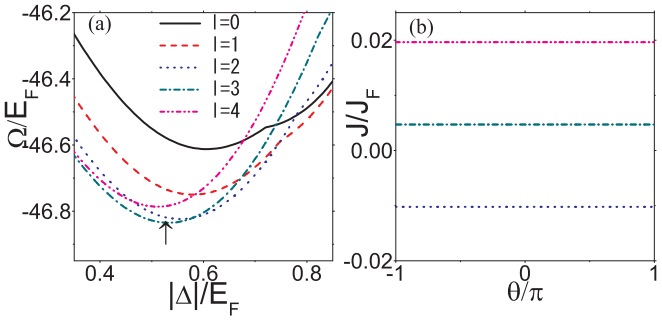

FIG. 5. Ring structure with uniform two-photon detuning. (a) The thermodynamic potential as a function of $|\Delta|$, with different angular momenta of the phase. The arrow shows the ground state. The parameters are $u_{\rm mag} = 0, \mu = -0.435E_F$; the other parameters are the same as in Fig. 3. (b) Spontaneous mass current for different l.

parameters shown in Fig. 5(a). For the local magnetic barrier, the FF phase $\exp(il_0\theta)$ changes across the barrier, leading to the tunable phase junction.

For the FF states in an infinite 1D homogeneous system, the mass current $J \propto \partial\Omega(Q)/\partial Q|_{Q=Q_0}$, with $\Omega(Q)$ being the thermodynamic potential for $\Delta(x) = \Delta_0 e^{iQx}$ and Q_0 being the center-of-mass momenta of Cooper pairs of the ground states. This current equals zero because $\partial\Omega/\partial Q|_{Q=Q_0} = 0$ is satisfied for the ground states [33,36]. However, in the ring-shaped system, instead of taking continuous values, the center-of-mass momenta Q can only take discrete values $Q = l/R$ due to the periodic boundary condition (note that the superposition of different l states is not energetically preferred). The value of the ground-state momenta Q_0 for the infinite system may not equal any Q in such a discrete set because Q_0 are determined by many parameters (pairing interaction, SOAM coupling strength, in-plane Zeeman field, etc.). Therefore $\partial\Omega(Q)/\partial Q|_{Q=l/R}$ can be nonzero for a finite ring-shaped system (i.e., $1/R \neq 0$), leading to finite mass current for the ground states. The direction of the current is also dictated by the sign of $\partial\Omega(Q)/\partial Q|_{Q=l/R}$. In Fig. 5(b), we plot the mass currents for three steady states corresponding to different values of l. They are all nonzero. The current of the ground state $l_0 = 3$ is smaller than other states with different l because of smaller $\partial\Omega(Q)/\partial Q|_{Q=l_0/R}$. The magnitude of the mass current depends on the difference between the ground-state momenta $Q = l_0/R$ in the ring and Q_0 in the infinite system, which does not explicitly depend on l_0. A smaller difference yields a smaller mass current. When $Q = Q_0$ accidentally, the mass current is zero as in the infinite case.

V. EXPERIMENTAL REALIZATION AND OBSERVATION

In experiments, we consider ^{40}K atoms and utilize LG laser beams to generate a ring trap as well as the SOAM coupling between two hyperfine states [44–47]. The magnetic barrier can be generated by a tightly focused laser beam [56]. When the wavelength of the focused laser lies between D_1 and D_2 transition lines, atoms at different hyperfine states experience different potentials, leading to a spin-dependent potential. To measure the current, one can sample one slice of the Fermi ring and measure its momentum distribution [57]. In this slice, the momentum difference of the atom cloud between the tangential direction of the ring and the opposite direction determines the local current. In addition, one can consider the Doppler-induced interference of the phonon modes, which has been utilized to measure the current in toroidal BECs [58]. Finally, because the mechanism for generating FF order parameters in the magnetic barrier is the same for one, two, and three dimensions [34,38], the proposed phase-tunable JJ should also apply to a 2D spin-orbit-coupled Fermi gas with a magnetic barrier line or a three-dimensional (3D) one with a magnetic barrier plane. In a ring trap, this means the radial confinement need not be very strong, corresponding to a 3D toroidal trap.

VI. SUMMARY

In summary, we proposed that the ground state of a Josephson junction with an arbitrary and tunable phase can be realized in spin-momentum-coupled Fermi superfluids in a harmonic trap or SOAM-coupled Fermi superfluids in a toroidal-shaped trap. When a phase different from the ground-state value is applied externally, it is known that a finite Josephson current is generated. We found that a spontaneous mass current exists in a finite ring-shaped system due to the periodic boundary condition, demonstrating the magnetoelectric effects in cold atoms. The experimental realization of such phase-tunable JJs may open novel possibilities for many applications in atomtronics, such as superfluid phase batteries and rectifiers, phase-based quantum bits, and the observation of topological superfluids and the associated Majorana fermions.

ACKNOWLEDGMENTS

We thank C. Wu for helpful discussions. This work is supported by ARO (Grant No. W911NF-12-1-0334), NSF (Grant No. PHY-1505496), and AFOSR (Grant No. FA9550-16-1-0387).

[1] A. Micheli, A. J. Daley, D. Jaksch, and P. Zoller, Phys. Rev. Lett. **93**, 140408 (2004).
[2] B. T. Seaman, M. Krämer, D. Z. Anderson, and M. J. Holland, Phys. Rev. A **75**, 023615 (2007).
[3] R. A. Pepino, J. Cooper, D. Z. Anderson, and M. J. Holland, Phys. Rev. Lett. **103**, 140405 (2009).
[4] R. Labouvie, B. Santra, S. Heun, S. Wimberger, and H. Ott, Phys. Rev. Lett. **115**, 050601 (2015).
[5] C. Ryu, P. W. Blackburn, A. A. Blinova, and M. G. Boshier, Phys. Rev. Lett. **111**, 205301 (2013).
[6] K. C. Wright, R. B. Blakestad, C. J. Lobb, W. D. Phillips, and G. K. Campbell, Phys. Rev. Lett. **110**, 025302 (2013).

[7] S. Eckel, J. G. Lee, F. Jendrzejewski, N. Murray, C. W. Clark, C. J. Lobb, W. D. Phillips, M. Edwards, and G. K. Campbell, Nature (London) **506**, 200 (2014).

[8] S. Gupta, K. W. Murch, K. L. Moore, T. P. Purdy, and D. M. Stamper-Kurn, Phys. Rev. Lett. **95**, 143201 (2005).

[9] C. Ryu, M. F. Andersen, P. Cladé, V. Natarajan, K. Helmerson, and W. D. Phillips, Phys. Rev. Lett. **99**, 260401 (2007).

[10] K. Henderson, C. Ryu, C. MacCormick, and M. G. Boshier, New J. Phys. **11**, 043030 (2009).

[11] A. Ramanathan, K. C. Wright, S. R. Muniz, M. Zelan, W. T. Hill, III, C. J. Lobb, K. Helmerson, W. D. Phillips, and G. K. Campbell, Phys. Rev. Lett. **106**, 130401 (2011).

[12] L. N. Bulaevskii, V. V. Kuzii, and A. A. Sobyanin, Pis'ma Zh. Eksp. Teor. Fiz. **25**, 314 (1977).

[13] O. Vávra, S. Gaži, D. S. Golubović, I. Vávra, J. Dérer, J. Verbeeck, G. Van Tendeloo, and V. V. Moshchalkov, Phys. Rev. B **74**, 020502 (2006).

[14] V. V. Ryazanov, V. A. Oboznov, A. Yu. Rusanov, A. V. Veretennikov, A. A. Golubov, and J. Aarts, Phys. Rev. Lett. **86**, 2427 (2001).

[15] V. B. Geshkenbein, A. I. Larkin, and A. Barone, Phys. Rev. B **36**, 235 (1987).

[16] C. C. Tsuei and J. R. Kirtley, Rev. Mod. Phys. **72**, 969 (2000).

[17] A. I. Larkin and Yu. N. Ovchinnikov, Sov. Phys. JETP **20**, 762 (1965).

[18] M. L. Kulić, Phys. Rev. A **76**, 053625 (2007).

[19] T. Kashimura, S. Tsuchiya, and Y. Ohashi, Phys. Rev. A **82**, 033617 (2010).

[20] A. A. Reynoso, G. Usaj, C. A. Balseiro, D. Feinberg, and M. Avignon, Phys. Rev. Lett. **101**, 107001 (2008).

[21] A. A. Reynoso, G. Usaj, C. A. Balseiro, D. Feinberg, and M. Avignon, Phys. Rev. B **86**, 214519 (2012).

[22] C. Padurariu and Y. V. Nazarov, Phys. Rev. B **81**, 144519 (2010).

[23] D. B. Szombati, S. Nadj-Perge, D. Car, S. R. Plissard, E. P. A. M. Bakkers, and L. P. Kouwenhoven, Nat. Phys. **12**, 568 (2016).

[24] Y.-J. Lin, R. L. Compton, K. Jiménez-García, J. V. Porto, and I. B. Spielman, Nature (London) **462**, 628 (2009).

[25] Y.-J. Lin, R. L. Compton, K. Jiménez-García, W. D. Phillips, J. V. Porto, and I. B. Spielman, Nat. Phys. **7**, 531 (2011).

[26] Y.-J. Lin, K. Jiménez-García, and I. B. Spielman, Nature (London) **471**, 83 (2011).

[27] J.-Y. Zhang, S.-C. Ji, Z. Chen, L. Zhang, Z.-D. Du, B. Yan, G.-S. Pan, B. Zhao, Y.-J. Deng, H. Zhai, S. Chen, and J.-W. Pan, Phys. Rev. Lett. **109**, 115301 (2012).

[28] C. Qu, C. Hamner, M. Gong, C. Zhang, and P. Engels, Phys. Rev. A **88**, 021604(R) (2013).

[29] A. J. Olson, S.-J. Wang, R. J. Niffenegger, C.-H. Li, C. H. Greene, and Y. P. Chen, Phys. Rev. A **90**, 013616 (2014).

[30] P. Wang, Z.-Q. Yu, Z. Fu, J. Miao, L. Huang, S. Chai, H. Zhai, and J. Zhang, Phys. Rev. Lett. **109**, 095301 (2012).

[31] L. W. Cheuk, A. T. Sommer, Z. Hadzibabic, T. Yefsah, W. S. Bakr, and M. W. Zwierlein, Phys. Rev. Lett. **109**, 095302 (2012).

[32] R. A. Williams, M. C. Beeler, L. J. LeBlanc, K. Jiménez-García, and I. B. Spielman, Phys. Rev. Lett. **111**, 095301 (2013).

[33] P. Fulde and R. A. Ferrell, Phys. Rev. **135**, A550 (1964).

[34] Z. Zheng, M. Gong, X. Zou, C. Zhang, and G. Guo, Phys. Rev. A **87**, 031602(R) (2013).

[35] F. Wu, G.-C. Guo, W. Zhang, and W. Yi, Phys. Rev. Lett. **110**, 110401 (2013).

[36] C. Qu, Z. Zheng, M. Gong, Y. Xu, L. Mao, X. Zou, G. Guo, and C. Zhang, Nat. Commun. **4**, 2710 (2013).

[37] W. Zhang and W. Yi, Nat. Commun. **4**, 2711 (2013).

[38] X.-J. Liu and H. Hu, Phys. Rev. A **88**, 023622 (2013).

[39] C. Chen, Phys. Rev. Lett. **111**, 235302 (2013).

[40] L. Dong, L. Jiang, and H. Pu, New J. Phys. **15**, 075014 (2013).

[41] Y. Xu, C. Qu, M. Gong, and C. Zhang, Phys. Rev. A **89**, 013607 (2014).

[42] X.-J. Liu, H. Jing, X. Liu, and M.-L. Ge, Eur. Phys. J. D **37**, 261 (2006).

[43] X.-J. Liu, X. Liu, L.-C. Kwek, and C. H. Oh, Front. Phys. China **3**, 113 (2008).

[44] M. DeMarco and H. Pu, Phys. Rev. A **91**, 033630 (2015).

[45] K. Sun, C. Qu, and C. Zhang, Phys. Rev. A **91**, 063627 (2015).

[46] C. Qu, K. Sun, and C. Zhang, Phys. Rev. A **91**, 053630 (2015).

[47] Y.-X. Hu, C. Miniatura, and B. Grémaud, Phys. Rev. A **92**, 033615 (2015).

[48] K.-P. Marzlin, W. Zhang, and E. M. Wright, Phys. Rev. Lett. **79**, 4728 (1997).

[49] M. F. Andersen, C. Ryu, P. Cladé, V. Natarajan, A. Vaziri, K. Helmerson, and W. D. Phillips, Phys. Rev. Lett. **97**, 170406 (2006).

[50] L. S. Leslie, A. Hansen, K. C. Wright, B. M. Deutsch, and N. P. Bigelow, Phys. Rev. Lett. **103**, 250401 (2009).

[51] S. Beattie, S. Moulder, R. J. Fletcher, and Z. Hadzibabic, Phys. Rev. Lett. **110**, 025301 (2013).

[52] X.-J. Liu, H. Hu, and P. D. Drummond, Phys. Rev. A **76**, 043605 (2007).

[53] X.-J. Liu, Phys. Rev. A **87**, 013622 (2013).

[54] L. Jiang, L. O. Baksmaty, H. Hu, Y. Chen, and H. Pu, Phys. Rev. A **83**, 061604(R) (2011).

[55] D. T. Colbert and W. H. Miller, J. Chem. Phys. **96**, 1982 (1992).

[56] C. Weitenberg, M. Endres, J. F. Sherson, M. Cheneau, P. Schausz, T. Fukuhara, I. Bloch, and S. Kuhr, Nature (London) **471**, 319 (2011).

[57] M. J. H. Ku, W. Ji, B. Mukherjee, E. Guardado-Sanchez, L. W. Cheuk, T. Yefsah, and M. W. Zwierlein, Phys. Rev. Lett. **113**, 065301 (2014).

[58] A. Kumar, N. Anderson, W. D. Phillips, S. Eckel, G. K. Campbell, and S. Stringari, New J. Phys. **18**, 025001 (2016).